Photocatalytic degradation of reactive black dye using ZnO – CeO2 Nanocomposites

Saravanan M.
SASTRA Deemed University
Vigneshwar S.
SASTRA Deemed University
Gautham B. Jegadeesan
SASTRA Deemed University
Ponnusami Venkatachalam (vponnu@chem.sastra.edu)
SASTRA Deemed University

Research Article

Keywords: Photocatalysis, ZnO, Ceria, Nanocomposites, Dye Degradation

Posted Date: September 8th, 2021

DOI: https://doi.org/10.21203/rs.3.rs-870597/v1

Abstract

Nano-CeO_2 was synthesized via the chemical precipitation of cerium precursor solution, and then mixed with nano-ZnO at various weight ratios to obtain ZnO-CeO_2nanocomposites. The composites were characterized for their morphological and photocatalytic properties. X-ray diffraction patterns of the pristine metal oxides corresponded well with (1 0 1) and (1 1 1) peaks of hexagonal wurtzite like-ZnO and cubic-phase CeO_2, respectively. The band gap of the ZnO-CeO_2nanocomposite was 3.08 eV, while that of pristine CeO_2 and ZnO powder was 3.24 eV and 3.12 eV respectively. Photocatalytic activity of ZnO-CeO_2composite was evaluated at various Reactive Black (RB) dye and catalyst concentrations. A 1:1 wt ratio ZnO-CeO_2 nanocompsite provided the maximum (~ 85%) RB oxidation under UV light within 90 minutes. Rate of dye degradation obtained with ZnO-CeO_2nanocomposite was almost 1.5 times more than that obtained with bare ZnO. It was observed that increase in CeO_2 to ZnO ratio increased oxidation rates up to 1:1 wt ratio. Increasing CeO_2 ratio beyond 1:1 wt. ratio did not significantly increase RB oxidation. The results confirm that addition of CeO_2 to ZnO has resulted in lowering its bandgap energy and in-turn favors oxidation of RB dye under UV light.

Introduction

Over the last two decades, there has been an increased emphasis on semi-conductor materials as photocatalysts for recalcitrant organic pollutant degradation (Bellardita et al. 2020; Chatterjee and Chakraborty 2021; Kurian 2020; Nagajyothi et al. 2020; Sar et al. 2018). Photodegradation reaction begins with absorption of light by the semiconductor photocatalysts resulting in the formation of electron-hole pairs. The charge carriers thus generated can initiate series of redox reactions upon reaching the surface of the catalysts. Thus, photocatalysts can be used in range of applications such as water treatment, fuel generation, synthetic chemistry etc. Photocatalysts such as ZnO and TiO_2 are commonly favored for water treatment due to their: (1) effectiveness; (2) ease in synthesis; (3) mechanical and thermal stability; (4) high specific surface area; (5) suitable bandgap and; (6) persistent generation of photo-generated carriers (Cai et al. 2017; Davis et al. 2019; Guan et al. 2021; Jo and Tayade 2014; Lee et al. 2016; Mahlambi et al. 2015; Ong et al. 2018; Pare et al. 2008). A significant body of research has shown that nano-ZnO, typically a hexagonal, wurtzite type semiconducting oxide, is highly effective in pollutant degradationbecause of its wide bandgap in the near-UV spectral region, and good photocatalytic property(Gu et al. 2016; Lee et al. 2016; Ratshiedana et al. 2021; Sanoop et al. 2016). ZnO can be easily processed at low temperatures to form nano-ZnO, which contains significant amounts lattice defects and oxygen vacancies in the crystal structures, and provides anisotropic growth which helps in increased photocatalysis (Gu et al. 2016). Even though a large number of photocatalysts had been developed in the recent years, commercial scale application of photocatalysts had been only limited due to poor efficiencies of these catalysts. Poor light absorption efficiency and recombination tendency of the electron-hole pair generated are the two important reasons for this.

To improve the photocatalytic efficiency, it is important to enhance the light absorption capacity of the photocatalyst and to prevent electron-hole pair recombination. One of the approaches is to form heterojunction between two semiconductors with favorable conduction band and valence band energy levels. In recent years, several metal, metal oxides and non-metal dopants have been developed to tune the band gap of ZnO (Gu et al. 2016; Meshram et al. 2017). Addition of metal and metal oxide impurities on ZnO induces defects in the ZnO nanostructures, reduces the bandgap energy levels, and expands its visible light response. Additionally, it can produce traps for photo-generated charge carries, thereby accelerating the charge transfer and inhibiting recombination of electron hole pairs(Bechambi et al. 2016; Caregnato et al. 2020; Jiang et al. 2017; Lang et al. 2016; Meshram et al. 2017; Parangusan et al. 2019). In recent years, ceria (CeO_2) is the most common rare-earth metal used due to its relative abundance, lower band gap (2.90–3.20 eV) compared to ZnO (3.10–3.30 eV), its chemical stability and tunable band gap (Arul et al. 2012; Bellardita et al. 2020; Davis et al. 2019; Kurian 2020; Meshram et al. 2017; Nagajyothi et al. 2020; Rajendran et al. 2016; Sane et al. 2018; Veedu et al. 2020). The redox pair of Ce^{3+}/Ce^{4+} acts as an electron scavenger, reducing recombination of electron-hole pair, and reducing the band gap. Upon doping 2 mol% Ce onto ZnO, 100% bisphenol A degradation was reported, which was 5–10 more than that observed for pristine ZnO (Bechambi et al. 2016). Meshram and his co-workers reported 99% crystal violet dye degradation using 4% doped Ce on ZnO within 100 minutes of sunlight irradiation (Meshram et al. 2017). They also observed that a 3-fold increase in photocatalytic activity of the Ce-doped ZnO, when compared to commercial pure ZnO. Maximum photocatalytic activity towards direct red-23 dye was observed with 3.28% Ce-doping on ZnO (Kumar et al. 2015). Increase in Ce doping beyond 3.28% reduced dye degradation moderately. In other studies, the optimum doping percent of Ce on ZnO nanoparticles was found to be 2–10% (Lang et al. 2016). Rajendran et al. observed a consistent decrease in the first-order degradation rate with increase in CeO_2 beyond 10 % (Rajendran et al. 2016). Upon use of 1:5 CeO_2:ZnO, 98% Rhodamine B degradation was observed in 180 minutes, compared to the 85% using the primary oxide, while 10% doping of CeO_2 on ZnO reduced methylene blue concentration by 67% in 150 minutes, again a 30% increase compared to the primary metal oxide photocatalyst (Lee et al. 2016).

In this work, a CeO_2-ZnOheterojunction nanocomposite was synthesized by mixing $CeO_2$and ZnO nanoparticles at various weight ratios. The morphological characteristics of the ZnO - CeO_2nanocomposite were determined. Reactive Black (RB) was used as the model dye compound to evaluate photocatalytic activity of the nanocomposite under UV-light illumination. With the exception of one study by Rajendran et al. (Rajendran et al. 2016), most studies have used less than 10 wt.% CeO_2 doped ZnO. Therefore, it is crucial to understand the effect of higher CeO_2 content on ZnO and its ability to influence the photocatalytic behavior of the composite. Additionally, the effect of process parameters such as dye concentration, catalyst amount and ZnO: CeO_2 weight ratios, and pH on photocatalytic ability of ZnO - CeO_2nanocompositewas evaluated to ascertain the efficacy of the nanocomposite under various operating parameters.

Experimental

Materials

Commercial nano-Zinc Oxide (ZnO, 99.9%) was purchased from Spectrum India Ltd. Sodium carbonate (Na_2CO_3) was purchased from Paxmy Specialty Chemicals, India. Cerium (IV) ammonium nitrate ($(NH4)_2Ce(NO_3)_6$), reactive black dye (RB, $C_{26}H_{21}N_5Na_4O_{19}S_6$), NaOH and H_2SO_4 were purchased from Avra Synthesis Ltd., India. All chemicals were of reagent grade and utilized as obtained. Double distilled water was used for material synthesis and photocatalytic experiments.

Synthesis of ZnO: Ceria Composites

Synthesis of cerium oxide (CeO_2) nanoparticles was adapted from previous studies (Lang et al. 2016; Ma et al. 2019; Nagajyothi et al. 2020; Sane et al. 2018). In 30 ml distilled water, 10 g cerium ammonium nitrate was added and kept for 30 minutes stirring. The as-prepared solution was added drop wise to 20 ml saturated solution of aqueous sodium carbonate with a pH of 9. A white precipitate was formed soon after cerium ammonium nitrate was added. Using stirring the formed precipitate was re-dissolved. By adding solid sodium carbonate, the ammonium carbonate solution was sustained at a pH of 9. The obtained slurry is centrifuged, and the wet product was calcined to 750^oC, and synthesized CeO_2nanoparticles were stored at room temperature. ZnO: CeO_2nanocomposites were prepared by adding appropriate quantities of nano-ZnO and nano-CeO_2 particles at varying weight ratios ranging from 1:4 to 2:1, hereby referred to as 1C1Z (1:1 CeO_2:ZnO),0.5C1Z (1:2 CeO_2:ZnO), 0.33C1Z (1:3 CeO_2:ZnO), 0.25C1Z (1:4 CeO_2:ZnO), 2C1Z (2:1 CeO_2:ZnO).

Material Characterization

X-Ray Diffraction (XRD) analysis of the nanoparticles was documented on a Focus X-ray Diffractometer (Bruker, Germany)**.** Debye-Scherrer formula was used to estimate the crystallite size of nanoparticles. Transmission electron microscopy (TEM, Hitachi) was used to determine the particle size and morphology of ZnO and CeO_2 nanoparticles. UV-visible diffuse reflectance spectra of ZnO and TiO_2 was carried out on a HACH UV-Vis spectrophotometer with a resolution of 5nm in the range of 200-900 nm, and the bandgap was determined using the Kubelka-Munk function. Reactive black dye (RB) was used as the model pollutant to determine the photocatalytic activity of ZnO: CeO_2 mixed oxides. The photo degradation studies were performed in a photochemical reactor set-up provided by SAIC India Ltd, Chennai, similar to the unit reported in our earlier study.

Photocatalytic Experiments

Experiments were done in a well type reactor of 100 ml capacity, with constant air circulation to ensure uniform mixing. Irradiation was provided using 30 W, 365 nm high pressure xenon long arc lamp. The concentration of RB investigated ranged from 250 mg/L – 1000 mg/L, with varying amounts of the ZnO: CeO_2 mixed oxides. It was ensured that the catalyst was well dispersed in solution, prior to the start of

the experiment. Control experiments in dark and non-aerated conditions with and without the catalyst were also performed to determine auto-degradation of RB dye. Parametric evaluation of the photocatalytic process was performed as followson the best performing ZnO: CeO_2 mixed oxide: (1) the effect of dye concentration ([RB] = 250 -1000 mg/L) using 1 g/ Lof nanoparticle; (2) the effect of nanoparticle loading (0.5-1.5 g/L) at RB concentration of 250-1000 mg/L; and (3) the effect of pH. Percent dye degradation was calculated according to Equation (1). Here C_0 is the initial concentration (mg/L) and $C_t$is the concentration (mg/L) at a given time. The kinetic study data obtained was fitted to pseudo-first order and pseudo-second order kinetic equations, commonly used to determine rate constants for photocatalytic processes, as shown in Equations (2) and (3), where k is the rate constant. DR-6000 UV-Vis spectrophotometer (HACH India) was used to determine RB dye concentration at a wavelength of 595 nm.

$$\%\ degradation, \eta = \frac{(C_o - C_t)}{C_o} \times 100 \quad (1)$$

$$ln\frac{C}{C_o} = -k_1 t \quad (2)$$

$$\frac{1}{C} - \frac{1}{C_o} = k_2 t \quad (3)$$

Result And Discussion

Morphology of ZnOand CeO_2 Nanoparticles

TEM images of nano-CeO_2 show that ceria nanoparticles were fairly well dispersed in solution, while nano-ZnO appeared more agglomerated (Fig.1a-d). Fig. 1e-f shows the powder X-ray diffraction patterns of ZnO & CeO_2nanoparticles. Nano-ZnO diffraction pattern corresponded well with hexagonal wurtzite structure with the diffraction peaks at (1 0 0), (1 0 1), (0 0 2), (1 0 2), (1 1 0), and (1 0 3) planes in good agreement with the standard hexagonal ZnO (JCPDS no. [75-0576]). XRD pattern for CeO_2 NPs corresponded well to that of CeO_2 standard JCPDS no. [65-5923], with peaks of (1 1 1), (2 0 0), (2 2 0), and (3 1 1) suggesting cubic-faced ceria nanoparticles.

The diffuse reflectance spectra of the ZnO and CeO_2 and 1:1 CeO_2: ZnO composite (1C1Z) is shown in Fig. 2 (a-c). The intercept of plot of photon energy (eV) versus $((R) * h\nu)^{1/2}$ (Kubelka-Munk function) revealed that the bandgap energy for ZnO& CeO_2 was 3.12 eV and 3.24 eV, respectively. The band gap energy obtained for CeO_2in this study was higher than that reported in other studies (Sane et al. 2018; Veedu et al. 2020). Upon addition of the ceria to the ZnO nanoparticles, the bandgap energy reduced to 3.08 eV. It can be noticed that addition of CeO_2 to ZnO helped decrease the band gap energy, which may result in an increased efficiency of the composite photocatalyst. Similar decrease in the band gap energy was observed by in other studies(Lang et al. 2016; Rodwihok et al. 2020; Veedu et al. 2020). Luo et al.

(Luo et al. 2020) noted that with 3% doping of CeO_2 on ZnO, the band gap energy reduced from 3.12 to 3.04 eV, and attributed the decrease to increased oxygen vacancies created upon addition on CeO_2, a rare-earth metal oxide found to be abundant in oxygen vacancies.

Photocatalytic Degradation of Reactive Black Dye

Control experiments were performed to evaluate the auto-degradation of RB dye. As seen in Fig. 3(a), degradation was negligible under dark conditions. In the presence of UV light and aeration, but absent the catalyst, less than 5% degradation was observed, most likely due to photolytic degradation of the dye (Kuo and Ho 2001). Addition of CeO_2 NPs to either an aerated or non-aerated dye solution showed insignificant dye degradation, suggesting no adsorption of RB on CeO_2 (Fig. 3a). However, when ZnO was added to both an aerated and non-aerated dye solution, in dark conditions, up to 7% dye removal was observed, indicating sorption.

Table 1. First order rate constant and percent degradation for various ZnO:CeO_2 composite

Catalyst Loading = 1 g/L									
Photocatalyst	**1000 mg/L**			**500 mg/L**			**250 mg/L**		
	k_1 (min^{-1})	**R^2**	**η (%)**	**k_1 (min^{-1})**	**R^2**	**η (%)**	**k_1 (min^{-1})**	**R^2**	**η (%)**
ZnO	0.009	0.99	56.3	0.047	0.99	96.3	0.113	0.99	99.1
Ceria	0.021	1.00	84.9	0.031	0.99	91.5	0.071	0.99	95.8
2C1Z	0.021	0.98	85.4	0.039	0.98	95.1	0.089	0.99	97.7
1C1Z	0.021	0.98	87.7	0.061	0.98	99.5	0.136	0.92	99.9
0.5C1Z	0.017	0.99	80.4	0.050	0.98	98.4	0.128	0.98	100.0
0.33C1Z	0.012	0.97	66.1	0.033	0.99	91.5	0.092	0.99	98.6
0.25C1Z	0.012	0.99	68.2	0.041	0.97	96.5	0.114	0.98	99.6

Fig. 3 (b & c) and Fig. 4 show the photocatalytic ability of various ZnO: CeO_2 wt. ratios on RB degradation at [RB] = 1000 mg/L and 1 g/L catalyst, and Table 1 shows the percent degradation. Within 90 minutes, > 60% degradation was observed with the use of different weight ratios of CeO_2 and ZnO nanoparticles. The absorbance spectra of RB decreased significantly within the first 15 minutes upon use of CeO_2-ZnO nanocomposites, with near complete degradation within 1 hour (Fig. 4).The degradation reached near equilibrium within 70 minutes and significantly reduced degradation rates was observed beyond reaction time of 70 minutes. The percent degradation was highest for 1C1Z (87.7%), while it was 80.4, 66.1, 68.2

% and 85.4% for 1C2Z, 0.33C1Z, 0.25C1Z, and 2C1Z respectively. Decreasing the amount of CeO_2 in the ZnO-CeO_2 heterojunction nanocomposite appeared to reduce RB degradation rates significantly (Table 1). Among the various wt. ratios of the composites investigated, IC!Z provided the maximum dye degradation. It is hypothesized that as the CeO_2 content is increased, efficient separation of electron-hole pair occurs favoring redox reactions on the surface, and hence increased percent degradation was observed.

Typically, photocatalytic degradation kinetics can best be described using first-order rate kinetics. Fig. 3c shows the plot of ln (C/C_0) vs. time for the various ZnO:CeO_2 nanocomposites. The first order plot clearly indicated that ZnO: CeO_2at 1:1 wt. ratio (1C1Z) performed the best among the various photocatalysts (Fig. 3c). The first order rate constants determined for 1C1Z was almost 3-fold higher than that for ZnO, and almost similar to pure CeO_2 at 1000 mg/L RB concentration and 1 g/L catalyst loading (Table 1). Increasing ZnO content in the composite decreased the first order rate constant, while increasing CeO_2 content increased it, largely due to the decrease in the band gap energy upon addition of CeO_2. The data was also fitted to a second order rate expression (Figure 5). The data fitted well to the pseudo-second order rate expression as well (quation 3, Table 2) at 1000 mg/L RB concentration and 1 g/L catalyst loading (R^2: 0.93 – 1.00). Sane et al. (Sane et al. 2018)reported better fit of a second order model to the kinetic data on the degradation of reactive dyes using CeO_2. The rate constants reported in their study ranged from 0.0085 – 0.016 L/mg min for the CeO_2 photocatalyst investigated for reactive dyes in the concentration range of 10-100 mg/L, slightly higher values of rate constant to the values obtained in our study.

Table 2. *Second order rate constant for various ZnO: CeO_2 composite*

Catalyst Loading = 1 g/L

Photocatalyst	**1000 mg/L**		**500 mg/L**		**250 mg/L**	
	k_2 x 10^{-5} (L- mg^{-1}-min^{-1})	**R^2**	**k_2 x 10^{-5} (L- mg^{-1}-min^{-1})**	**R^2**	**k_2 x 10^{-5} (L- mg^{-1}-min^{-1})**	**R^2**
ZnO	1.40	0.98	64.39	0.85	1040.76	0.81
Ceria	5.60	0.93	23.02	0.86	168.94	0.80
2C1Z	6.36	0.98	46.32	0.89	333.68	0.76
1C1Z	6.97	0.94	274.68	0.51	5204.00	0.33
0.5C1Z	4.26	0.98	97.81	0.57	766.77	0.61
0.33C1Z	2.24	1.00	26.73	0.88	525.50	0.72
0.25 C1Z	2.20	0.98	52.04	0.66	1414.63	0.55

Effect of Initial Dye Concentration

The effect of initial dye concentration on degradation rates was examined. Fig. 6 and 7 show the kinetic data and the respective first-order kinetic plots for RB concentration of 500 mg/L (6a & b) and 250 mg/L (7 a & b), at 1 g/L catalyst loading, respectively. In about 75 minutes, greater than 90% degradation was observed for various weight ratios of CeO_2 and ZnO nanoparticles. Similar to that observed for 1000 mg/L RB concentration, decreasing CeO_2 content in the nanocomposite decreased percent degradation, albeit marginally for an initial concentration of 500 mg/L (Fig. 6). The degradation kinetics clearly fitted to first order rate expression with high R^2 values, but appeared to be poorer fits for second-order rate expressions (Table 2). As the initial RB concentration is lowered to 250 mg//L, percent removal increased to near 100% (Fig. 7a). Similar to the previous observation, the data fitted better to first-order rate expressions, rather than second-order rate expressions (Fig. 7b). Similarly, increasing CeO_2 fraction on ZnO did not significantly improve the percent degradation since near complete degradation was observed for all photocatalysts used within 45 minutes (Fig. 7a). Equilibrium was also obtained within 45 minutes with negligible change in rate of degradation after 30 minutes. Although degradation rate was slower for CeO_2 and 1C1Z initially, the degradation rate of 1C1Z after 45 minutes was comparable with that of ZnO photocatalysts. Decrease in the initial RB concentration resulted in faster degradation, as observed by a 2-5 fold increase in the first order rate constant (Table 2). For 1C1Z, the rate constant amplified almost 6 times from 0.021 to 0.136 min^{-1} as RB concentration decreased from 1000 to 250 mg/L. It was observed generally that as initial RB concentration decrease, the rate constant and therefore the initial rate (kC_o) increased. For the same number of reactive sites on the surface, decrease in [RB] moieties due to decreasing initial concentration results in increased adsorption on the surface and increased degradation. At higher concentration, there is competition for the reactive sites, hence the initial rate is lowered. In all the experiments with varying RB concentrations and ZnO: CeO_2 weight ratios, 1C1Z exhibited the highest degradation rate, with the first order rate constant almost twice as high as that of pure ZnO.

Effect of Catalyst Loading

To further evaluate the photocatalytic process, kinetic experiments were performed at varying catalytic loadings using the best performing photocatalyst, 1C1Z, and its efficacy compared to that of pristine nano-ZnO and nano-CeO_2. Fig.8 (a-c) shows the kinetic data for catalyst loading of 0.5 g/L (RB concentration = 250 – 1000 mg/L) and Fig.8 (d-f) shows the kinetic data for catalyst loading of 1.5 g/L (RB concentration = 250 – 1000 mg/L). Table 3 presents the percent degradation and constants to the first – order data fit. For 250 and 500 gm/L RB concentration (Fig. 8), there was no appreciable difference in degradation rate among the three photocatalysts investigated, ZnO and CeO_2 and 1C1Z. Near complete degradation was observed within 60 minutes, particularly at low concentrations. At low catalyst loading (0.5 g/L) and high RB concentration, the degradation rates were lower. Equilibrium was not attained within 50 minutes for 1000 mg/L and 500 mg/L RB concentration, while it was observed with 250 mg/L RB concentration. The percent degradation was 35-40% for 1000 mg/L, 60-65% for 500 mg/L and almost 100 % for 250 mg/L, at 0.5 g/L. The percent degradation was 55-60% for 1000 mg/L, 85-95% for 500

mg/L and almost 100 % for 250 mg/L, at 1.5 g/L. As the catalyst loading was increased, degradation rates were faster as evidenced by the near complete completion in lesser reaction times. Increasing catalyst loading increased percent removals and degradation rates as there is an expected rise in the number of reactive sites.

The data was fitted to first-order rate expression, and the rate constant deduced. The first order rate constant for degradation of dye by ZnO was observed to be 0.008 min^{-1} (R^2 =0.953), while it was 0.01 min^{-1} (R^2= 0.983) and 0.007 min^{-1} (R^2 =0.988) using CeO_2 and 1C1Z respectively for RB concentration of 1000 mg/L. Similarly, for 500 mg/L RB dye concertation the first order rate constants were found to be 0.027 min^{-1} (R^2 = 0.993), 0.027 min^{-1} (R^2 = 0.992) and 0.019 (R^2 = 0.984) for ZnO, CeO_2 and 1C1Z respectively. Correspondingly, the first order rate constants for 250 mg/L RB dye concentration provided the values of 0.106 min^{-1} (R^2 = 0.933), 0.07 min^{-1} (R^2 = 0.978) and 0.04 (R^2 = 0.99) for ZnO, CeO_2 and 1C1Z respectively.

Table 3. *First order rate constant and percent degradation for various catalyst loadings*

Catalyst Loading = 0.5 g/L									
Photocatalyst	**1000 mg/L**			**500 mg/L**			**250 mg/L**		
	k_1 (min^{-1})	**R^2**	**η (%)**	**k_1 (min^{-1})**	**R^2**	**η (%)**	**k_1 (min^{-1})**	**R^2**	**η (%)**
ZnO	0.008	0.95	47.5	0.027	0.99	85.8	0.104	0.95	99.1
Ceria	0.010	0.98	60.9	0.027	0.99	89.0	0.070	0.98	97.5
1C1Z	0.007	0.99	42.1	0.019	0.98	79.2	0.040	0.99	82.9
Catalyst Loading = 1.5 g/L									
Photocatalyst	**1000 mg/L**			**500 mg/L**			**250 mg/L**		
	k_1 (min^{-1})	**R^2**	**η (%)**	**k_1 (min^{-1})**	**R^2**	**η (%)**	**k_1 (min^{-1})**	**R^2**	**η (%)**
ZnO	0.018	0.99	78.4	0.050	0.99	98.1	0.143	0.95	99.6
Ceria	0.026	0.98	91.6	0.066	0.99	99.2	0.073	0.88	98.5
1C1Z	0.017	0.98	75.8	0.037	0.99	96.1	0.138	0.96	99.7

Table 3 presents the rate constant for a catalyst loading of 1.5 g/L. It can be seen that increasing loading three times increased the rate constant also 3 fold, for 1000 mg/L. However, when the initial RB concentration was 250 mg/L, the rate constant remained constant or marginally increased. This suggested that RB concentration was the rate controlling factor when the number of reactive sites was in

abundance.The results from this study were compared to results from studies wherein binary metal oxide photocatalysts were used for dye degradation. As seen in Table 4, when ZnO: $CeO_2$was used in a ratio of 1:5 for Rhodamine degradation, the efficiency was 98%, albeit at low dye concentration (24 mg/L). Similar efficiencies were reported when the base material ZnO was doped with other metal oxides such as Bi_2O_3, CdO etc. It has also been noted that doping a second metal oxide on ZnO significantly improved degradation efficiencies, as is the case here.

Table 4. *Comparison of results to reported studies*

Photocatalyst	Experimental condition	Degradation efficiency %		Reference
		ZnO	Binary	
CuO/ZnO	CuO/ZnO = 2 g/L [MO] = 20 mg/L; Irradiation time = 60 min	50.0	90.0	(Liu et al. 2008)
CdS/ZnO (1:3)	CdS/ZnO = 0.5 g/L [RhB] = 24 mg/L Irradiation time = 90 min	~ 45.0	100	(Li et al. 2011)
CeO_2/ZnO (1:5)	CeO_2/ZnO = 0.5 g/L [RhB] = 24 mg/L Irradiation time = 180 min	82.3	98	(Li et al. 2011)
Bi_2O_3/ZnO (1:23)	Bi_2O_3/ZnO = 1 g/L [RhB] = 4.8 mg/L Irradiation time = 180 min	~ 15.0	85.0	(Yang et al. 2014)
CdO/ZnO (10 wt.% CdO)	CdO/ZnO = N/A [MB] = NA mg/L Irradiation time = 360 min	4.9	49.7	(Saravanan et al. 2015)
CeO_2/ZnO (10:90)	CeO_2/ZnO = NA [RhB] = 1000 mg/L Irradiation time = 150 min	4.2	95.9	(Rajendran et al. 2016)
Mg/ZnO (7.5 wt% Mg)	Mg/ZnO = 50 mg/L [RhB] = 20 mg/L Irradiation time = 120 min	15.0	75.0	(Pradeev raj et al. 2018)
CeO_2/ZnO (1:1)	CeO_2/ZnO = 1 g/L [RB] = 1000 mg/L Irradiation time = 90min	56.3	87.7	Our work

Effect of pH on RB degradation

The effect of pH on RB degradation was evaluated on the best performing photocatalyst, 1C1Z at various solution pH and the its efficacy compared to that of pristine nano-ZnO and nano-CeO_2. Here, the effect of pH was performed at 1000 mg/L dye concentration and 1 g/L catalyst loading (Fig. 9). In the acidic pH region, degradation efficiencies were very low (< 30%) for all the photocatalysts investigated. However, as pH was increased to 11, higher degradation of 99%,98% and 47% was observed for 1ClZ, ZnO and CeO_2respectively. Previous research has shown that photocatalytic reactions are pH-dependent, primarily caused by the surface charge of the catalyst and the molecular structure of the organic contaminant. The increase in percent degradation at higher pH can be attributed to the increase in the number of hydroxyl ions. The pKa value for reactive black dye is 3.8 and 6.9. The pH at point of zero charge (pH_{PZC}) for CeO_2 has been reported to be 6.9 while that for ZnO has been 8.7-9.7 (Meshram et al. 2017). Since RB is an anionic dye, electrostatic attraction between the dye molecule and catalyst surface at pH <pH_{PZC} results in the dye removal at acidic pH. Since the pH_{PZC} shifts towards more alkaline pH in a ZnO: CeO_2 mixture, higher percent removals are expected. Sane et al. (Sane et al. 2018) reported that activity of CeO_2 for dye degradation was higher at neutral pH, and followed the order: 7 > 9.2 > 4. However, when ZnO based catalysts were used for degradation of Rhodamine – B dye, higher pH provided the best degradation (Saffari et al. 2020). Highest percentage removal of dye was observed at a pH of 11. Among all the photocatalyst studied, 1C1Z performed the best, clearly indicating that the addition of CeO_2 to ZnO significantly improved the photocatalytic activity of the composite.

Conclusion

In this work, ZnO: CeO_2heterojunctionnanocatalysts were synthesized and tested for their photocatalytic activity with reactive black dye. Maximum dye degradation was obtained with a ZnO: CeO_2composite of 1:1 wt ratio (1C1Z), wherein over 85% removal at RB concentrations of 1000 mg/L was observed. Addition of cerium to ZnO reduces band gap of ZnO and helps charge-carrier separation, thereby resulting in increased degradation rates by 1.5 times. Beyond 1:1 wt ratio of ZnO: CeO_2, no significant increase in RB degradation was observed. The kinetic data fitted well to first-order kinetics. Increase in catalyst loading increased degradation rates, while increased concentration decreased it. At pH greater than 9, almost complete degradation was observed. This study emphasizes that doping ceria on ZnO up to 1:1 ratio is an effective way to degrade dyes by photocatalysis under alkaline pH conditions.

Declarations

Acknowledgements

The authors acknowledge the support of SASTRA Deemed University for providing infrastructure facilities required to complete this work.

Conflict of interest

This work has not received any financial support

Funding

This work has not received any financial support

Availability of Data and Materials

The datasets generated during the current study are available from the corresponding author on reasonable request.

Code Availability

Not applicable

Authors' contributions

M. Saravanan: Investigation, Validation, Writing - Original Draft

S. Vigneshwar: Investigation

Gautham B. Jegadeesan: Conceptualization, Resources, Supervision, Formal analysis, Visualization

V. Ponnusami: Supervision, Visualization, Writing - Review & Editing

References

1. Arul, N. S. *et al.* Enhanced photocatalytic activity of cobalt-doped CeO2 nanorods. *Journal of Sol-Gel Science and Technology*, **64** (3), 515–523 https://doi.org/10.1007/s10971-012-2883-7 (2012).
2. Bechambi, O., Jlaiel, L., Najjar, W. & Sayadi, S. Photocatalytic degradation of bisphenol A in the presence of Ce-ZnO: Evolution of kinetics, toxicity and photodegradation mechanism. *Materials Chemistry and Physics*, **173**, 95–105 https://doi.org/10.1016/j.matchemphys.2016.01.044 (2016).
3. Bellardita, M., Fiorenza, R., Palmisano, L. & Scirè, S. (2020). Photocatalytic and photothermocatalytic applications of cerium oxide-based materials. Cerium Oxide (CeOâ„): Synthesis, Properties and Applications. (pp. 109–167). Elsevier. https://doi.org/10.1016/b978-0-12-815661-2.00004-9
4. Cai, Z. *et al.* An overview of nanomaterials applied for removing dyes from wastewater. *Environmental Science and Pollution Research*, **24** (19), 15882–15904 https://doi.org/10.1007/s11356-017-9003-8 (2017).
5. Caregnato, P., Jiménez, K. R. E. & Villabrille, P. I. Ce-doped ZnO as photocatalyst for carbamazepine degradation. *Catal. Today*, **372**, 183–190 https://doi.org/10.1016/j.cattod.2020.07.031 (2021).
6. Chatterjee, P. & Chakraborty, A. K. Metal organic framework derived Ca4Fe9O17 as photocatalyst for degradation of organic dyes. *Mater. Lett*, **284**, 129034 https://doi.org/10.1016/j.matlet.2020.129034 (2021).

7. Davis, K., Yarbrough, R., Froeschle, M., White, J. & Rathnayake, H. Band gap engineered zinc oxide nanostructures: Via a sol-gel synthesis of solvent driven shape-controlled crystal growth. *RSC Advances*, **9** (26), 14638–14648 https://doi.org/10.1039/c9ra02091h (2019).
8. Gu, X. *et al.* ZnO based heterojunctions and their application in environmental photocatalysis., **27** (40), 402001 https://doi.org/10.1088/0957-4484/27/40/402001 (2016).
9. Guan, S. *et al.* Enhanced photocatalytic activity and stability of TiO2/graphene oxide composites coatings by electrophoresis deposition. *Mater. Lett*, **286**, 129258 https://doi.org/10.1016/j.matlet.2020.129258 (2021).
10. Jiang, J. *et al.* Porous Ce-doped ZnO hollow sphere with enhanced photodegradation activity for artificial waste water. *Journal of Alloys and Compounds*, **699**, 907–913 https://doi.org/10.1016/j.jallcom.2017.01.036 (2017).
11. Jo, W. K. & Tayade, R. J. New generation energy-efficient light source for photocatalysis: LEDs for environmental applications. *Industrial and Engineering Chemistry Research*, **53** (6), 2073–2084 https://doi.org/10.1021/ie404176g (2014).
12. Kumar, R. *et al.* Ce-doped ZnO nanoparticles for efficient photocatalytic degradation of direct red-23 dye. *Ceram. Int*, **41** (6), 7773–7782 https://doi.org/10.1016/j.ceramint.2015.02.110 (2015).
13. Kuo, W. S. & Ho, P. H. Solar photocatalytic decolorization of methylene blue in water., **45** (1), 77–83 https://doi.org/10.1016/S0045-6535(01)00008-X (2001).
14. Kurian, M. Cerium oxide based materials for water treatment-A review. *Journal of Environmental Chemical Engineering*, **8** (5), 104439 https://doi.org/10.1016/j.jece.2020.104439 (2020).
15. Lang, J. *et al.* Chemical precipitation synthesis and significant enhancement in photocatalytic activity of Ce-doped ZnO nanoparticles. *Ceram. Int*, **42** (12), 14175–14181 https://doi.org/10.1016/j.ceramint.2016.06.042 (2016).
16. Lee, K. M., Lai, C. W., Ngai, K. S. & Juan, J. C. Recent developments of zinc oxide based photocatalyst in water treatment technology: A review. *Water Res*, **88**, 428–448 https://doi.org/10.1016/j.watres.2015.09.045 (2016).
17. Li, C. *et al.* Electrospinning of CeO2–ZnO composite nanofibers and their photocatalytic property. *Mater. Lett*, **65** (9), 1327–1330 https://doi.org/10.1016/j.matlet.2011.01.075 (2011).
18. Liu, Z. L., Deng, J. C., Deng, J. J. & Li, F. F. Fabrication and photocatalysis of CuO/ZnO nano-composites via a new method. *Materials Science and Engineering: B*, **150** (2), 99–104 https://doi.org/10.1016/j.mseb.2008.04.002 (2008).
19. Luo, K. *et al.* Synthesizing CuO/CeO2 /ZnO ternary nano-photocatalyst with highly effective utilization of photo-excited carriers under sunlight. *Nanomaterials*, **10** (10), 1–13 https://doi.org/10.3390/nano10101946 (2020).
20. Ma, R. *et al.* A critical review on visible-light-response CeO2-based photocatalysts with enhanced photooxidation of organic pollutants. *Catal. Today*, **335**, 20–30 https://doi.org/10.1016/j.cattod.2018.11.016 (2019).

21. Mahlambi, M. M. *et al.* (2015). TiO_2 Nanocatalysts Supported on a Hybrid Carbon-Covered Alumina Support: Comparison between Visible Light and UV Light Degradation of Rhodamine B. Journal of Nanotechnology, vol. 2015, Article ID 198723, 8 pages. https://doi.org/10.1155/2015/198723
22. Meshram, S. P., Adhyapak, P. V., Pardeshi, S. K., Mulla, I. S. & Amalnerkar, D. P. Sonochemically generated cerium doped ZnO nanorods for highly efficient photocatalytic dye degradation. *Powder Technol*, **318**, 120–127 https://doi.org/10.1016/j.powtec.2017.05.044 (2017).
23. Nagajyothi, P. C. *et al.* Green synthesis: Photocatalytic degradation of textile dyes using metal and metal oxide nanoparticles-latest trends and advancements. *Critical Reviews in Environmental Science and Technology*, **50** (24), 2617–2723 https://doi.org/10.1080/10643389.2019.1705103 (2020).
24. Ong, C. B., Ng, L. Y. & Mohammad, A. W. A review of ZnO nanoparticles as solar photocatalysts: Synthesis, mechanisms and applications. *Renewable and Sustainable Energy Reviews*, **81**, 536–551 https://doi.org/10.1016/j.rser.2017.08.020 (2018).
25. Parangusan, H., Ponnamma, D. & Al-Maadeed, M. A. A. Effect of cerium doping on the optical and photocatalytic properties of ZnO nanoflowers. *Bulletin of Materials Science*, **42** (4), 1–11 https://doi.org/10.1007/s12034-019-1865-6 (2019).
26. Pare, B., Jonnalagadda, S. B., Tomar, H., Singh, P. & Bhagwat, V. W. ZnO assisted photocatalytic degradation of acridine orange in aqueous solution using visible irradiation., **232** (1–3), 80–90 https://doi.org/10.1016/j.desal.2008.01.007 (2008).
27. Pradeev raj, K. *et al.* Influence of Mg Doping on ZnO Nanoparticles for Enhanced Photocatalytic Evaluation and Antibacterial Analysis. *Nanoscale Res. Lett*, **13** (1), 229 https://doi.org/10.1186/s11671-018-2643-x (2018).
28. Rajendran, S. *et al.* Ce3+-ion-induced visible-light photocatalytic degradation and electrochemical activity of ZnO/CeO2 nanocomposite. *Sci. Rep*, **6** (1), 31641 https://doi.org/10.1038/srep31641 (2016).
29. Ratshiedana, R., Kuvarega, A. T. & Mishra, A. K. Titanium dioxide and graphitic carbon nitride–based nanocomposites and nanofibres for the degradation of organic pollutants in water: a review. *Environmental Science and Pollution Research*, **28** (9), 10357–10374 https://doi.org/10.1007/s11356-020-11987-3 (2021).
30. Rodwihok, C. *et al.* Cerium-oxide-nanoparticle-decorated zinc oxide with enhanced photocatalytic degradation of methyl orange. *Applied Sciences (Switzerland)*, **10** (5), https://doi.org/10.3390/app10051697 (2020).
31. Saffari, R., Shariatinia, Z. & Jourshabani, M. Synthesis and photocatalytic degradation activities of phosphorus containing ZnO microparticles under visible light irradiation for water treatment applications. *Environ. Pollut*, 259 https://doi.org/10.1016/j.envpol.2019.113902 (2020).
32. Sane, P. K., Tambat, S., Sontakke, S. & Nemade, P. Visible light removal of reactive dyes using CeO2 synthesized by precipitation. *Journal of Environmental Chemical Engineering*, **6** (4), 4476–4489 https://doi.org/10.1016/j.jece.2018.06.046 (2018).

33. Sanoop, P. K. *et al.* Synthesis of yttrium doped nanocrystalline ZnO and its photocatalytic activity in methylene blue degradation. *Arabian Journal of Chemistry*, **9**, S1618–S1626 https://doi.org/10.1016/j.arabjc.2012.04.023 (2016).
34. Sar, S. K. *et al.* Study of uranium level in groundwater of Balod district of Chhattisgarh state, India and assessment of health risk. *Human and Ecological Risk Assessment*, **24** (3), 691–698 https://doi.org/10.1080/10807039.2017.1397498 (2018).
35. Saravanan, R. *et al.* ZnO/Ag/CdO nanocomposite for visible light-induced photocatalytic degradation of industrial textile effluents. *Journal of Colloid and Interface Science*, **452**, 126–133 https://doi.org/10.1016/j.jcis.2015.04.035 (2015).
36. Veedu, S. N., Jose, S., Narendranath, S. B., Prathapachandra Kurup, M. R. & Periyat, P. Visible light-driven photocatalytic degradation of methylene blue dye over bismuth-doped cerium oxide mesoporous nanoparticles. *Environmental Science and Pollution Research*, **28** (4), 4147–4155 https://doi.org/10.1007/s11356-020-10750-y (2020).
37. Yang, Y. *et al.* (2014). Electrospun ZnO/Bi2O3 nanofibers with enhanced photocatalytic activity. Journal of Nanomaterials, vol. 2014, Article ID 130539, 7 pages 130539. https://doi.org/10.1155/2014/130539

Figures

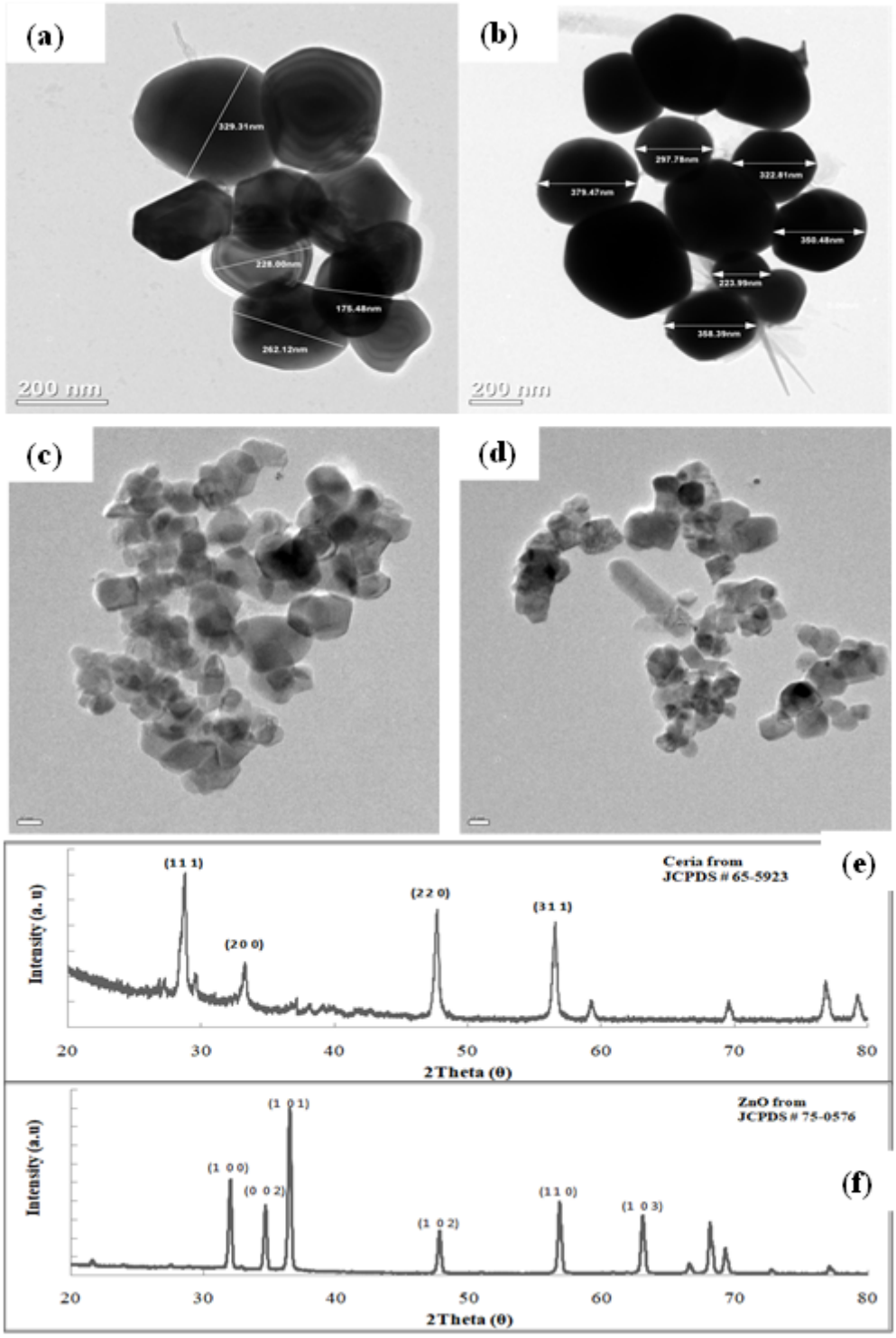

Figure 1

Characterization of as-prepared CeO2 and ZnO: (a) & (b) – TEM images of as-prepared CeO2; (c) & (d) - TEM images of as-prepared ZnO; (e) & (f) – XRD patterns of CeO2 and ZnO

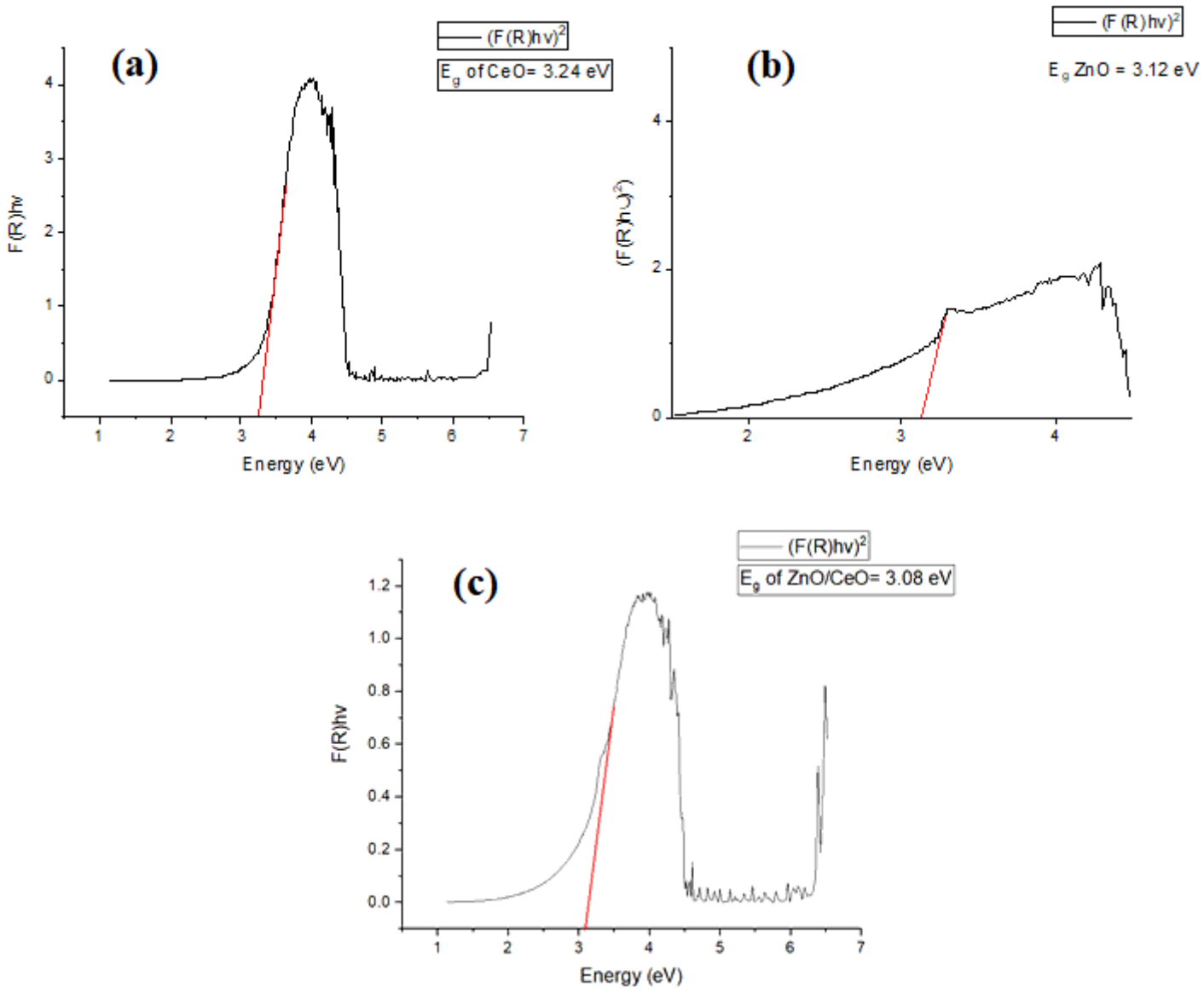

Figure 2

UV-NIR spectra of (a) Ceria; (b) ZnO and; (c) Ceria: ZnO (1:1 wt. ratio). The bandgap energy was calculated using the Kubelka-Munk function.

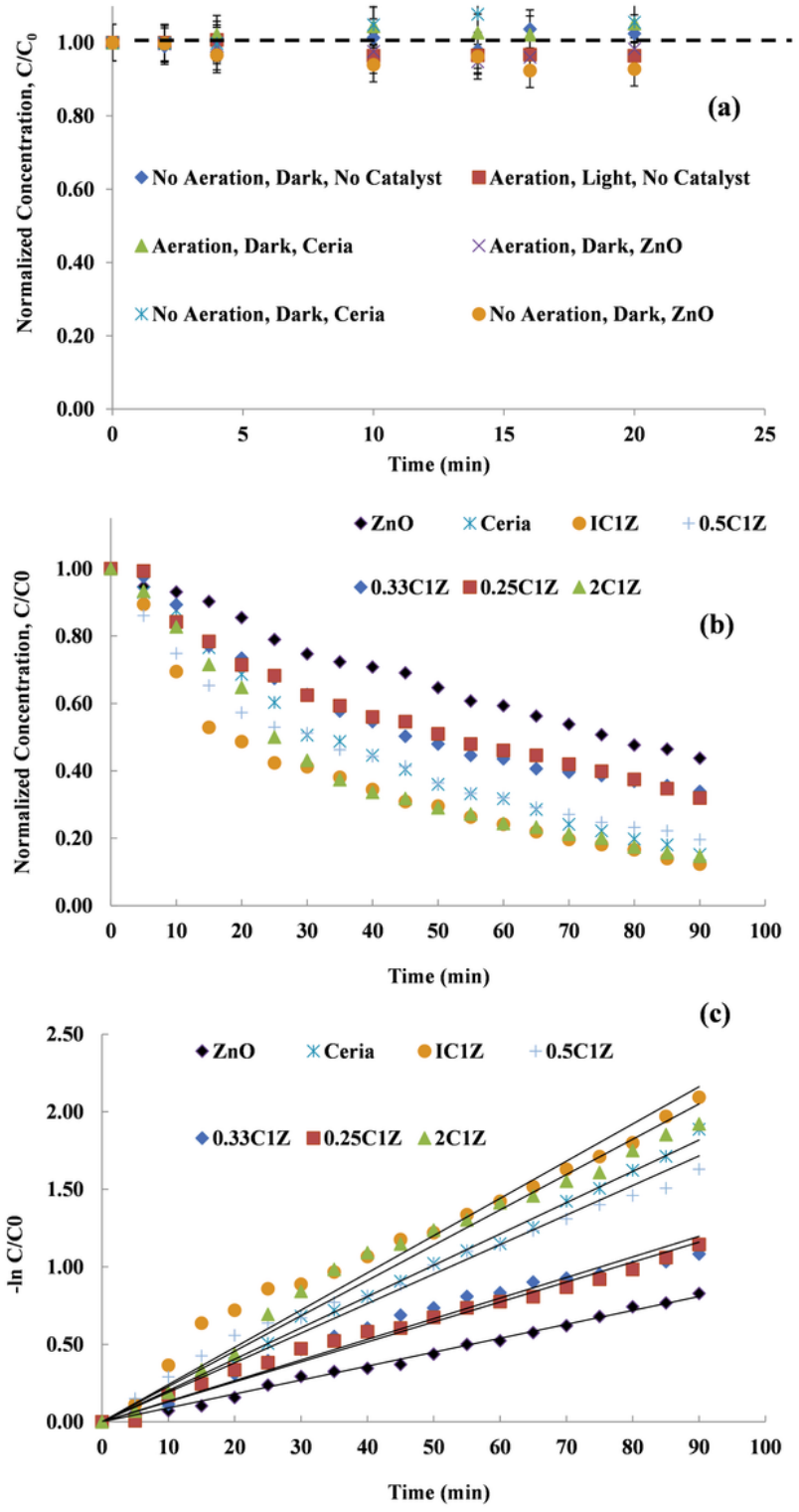

Figure 3

UV-NIR spectra of (a) Ceria; (b) ZnO and; (c) Ceria: ZnO (1:1 wt. ratio). The bandgap energy was calculated using the Kubelka-Munk function.

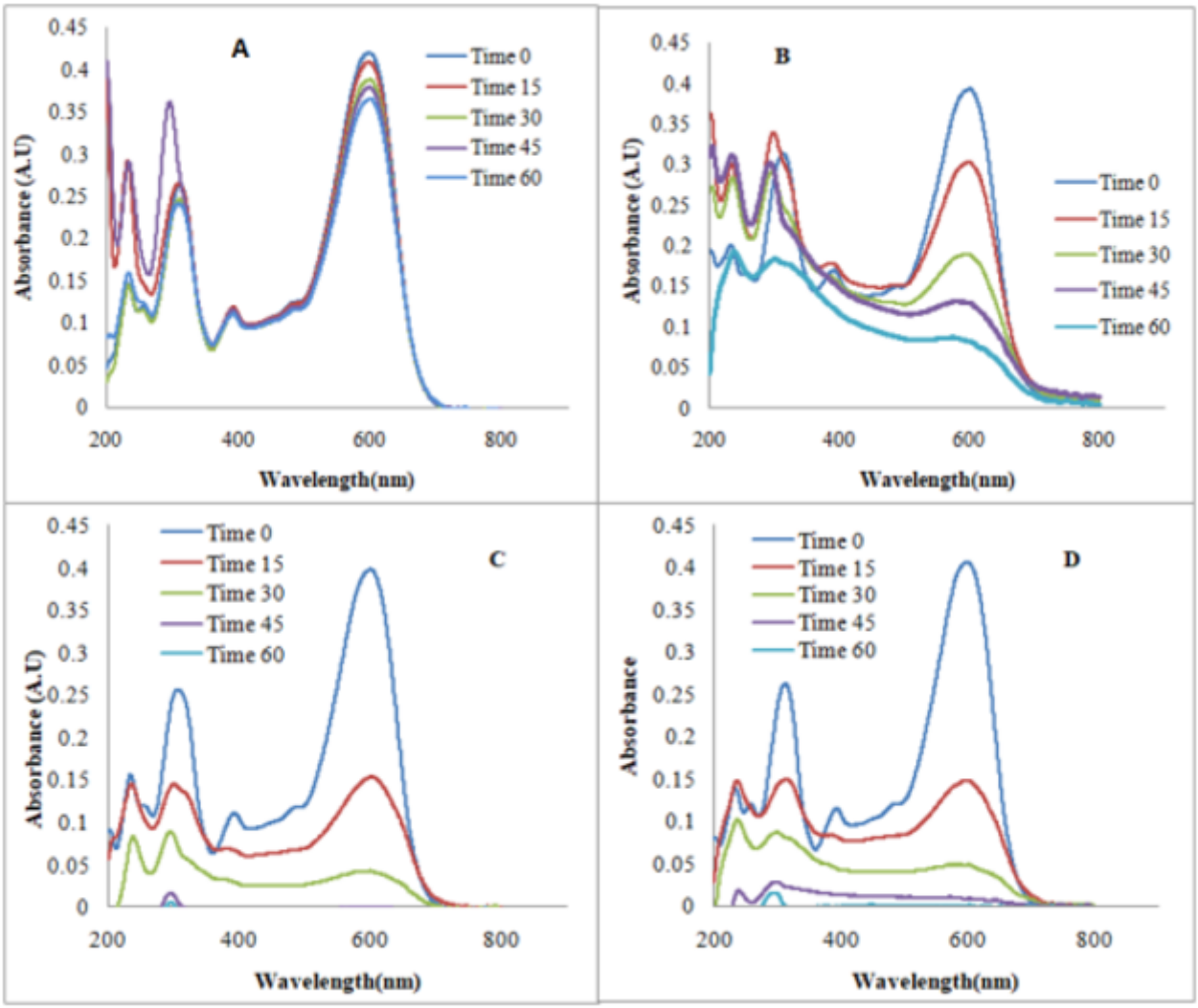

Figure 4

UV-Vis absorption spectra on dye degradation upon photocatalysis: (A) Reactive black control; (B) Ceria; (C) ZnO and (D) Ceria:ZnO – 1:1 wt ratio.

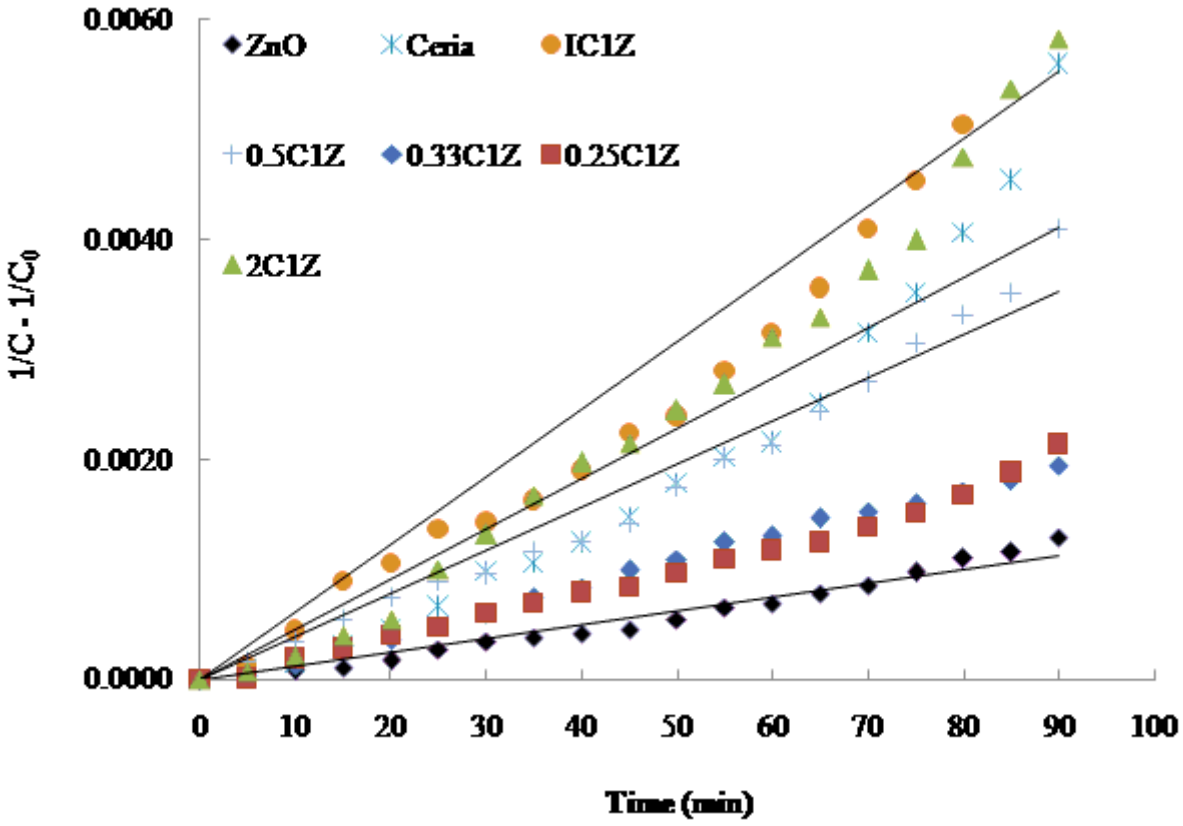

Figure 5

UV-Vis absorption spectra on dye degradation upon photocatalysis: (A) Reactive black control; (B) Ceria; (C) ZnO and (D) Ceria:ZnO – 1:1 wt ratio.

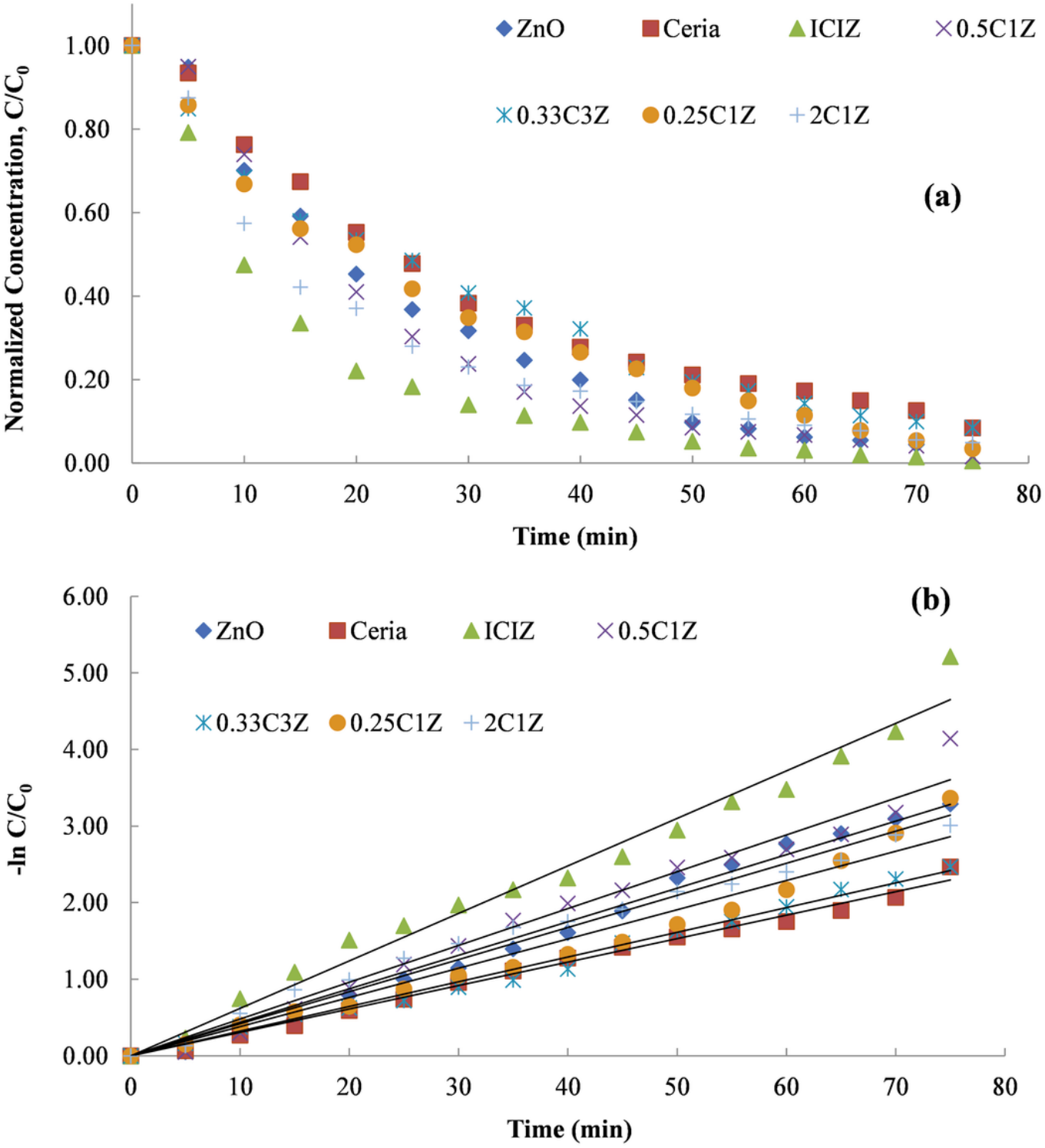

Figure 6

(a) Effect of CeO2 content in ZnO: CeO2 composite on RB degradation for RB=500 mg/L, catalyst = 1 g/L; and (b) data fit to first-order rate expression.

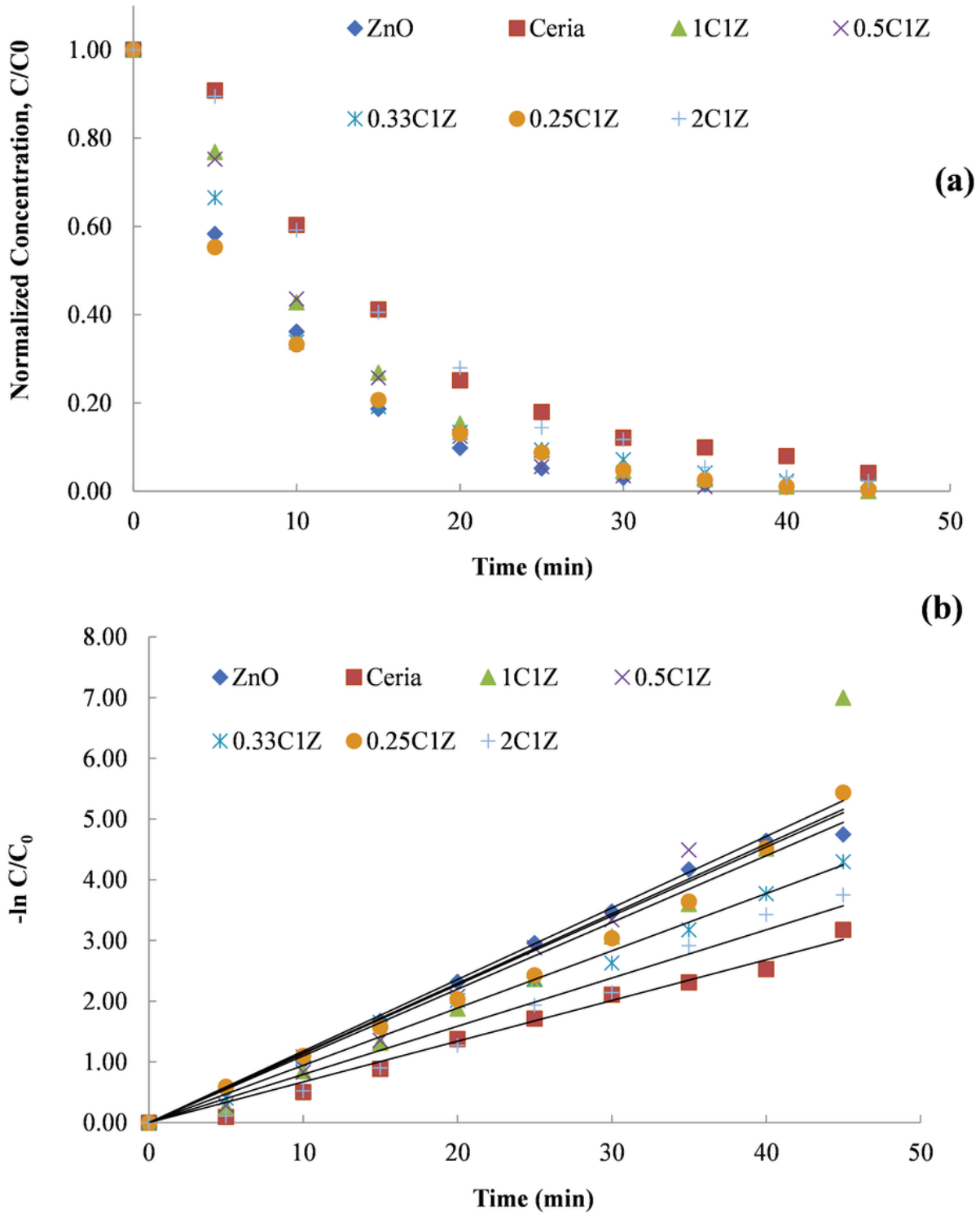

Figure 7

(a) Effect of CeO2 content in ZnO: CeO2 composite on RB degradation for RB=250 mg/L, catalyst = 1 g/L; and (b) data fit to first-order rate expression.

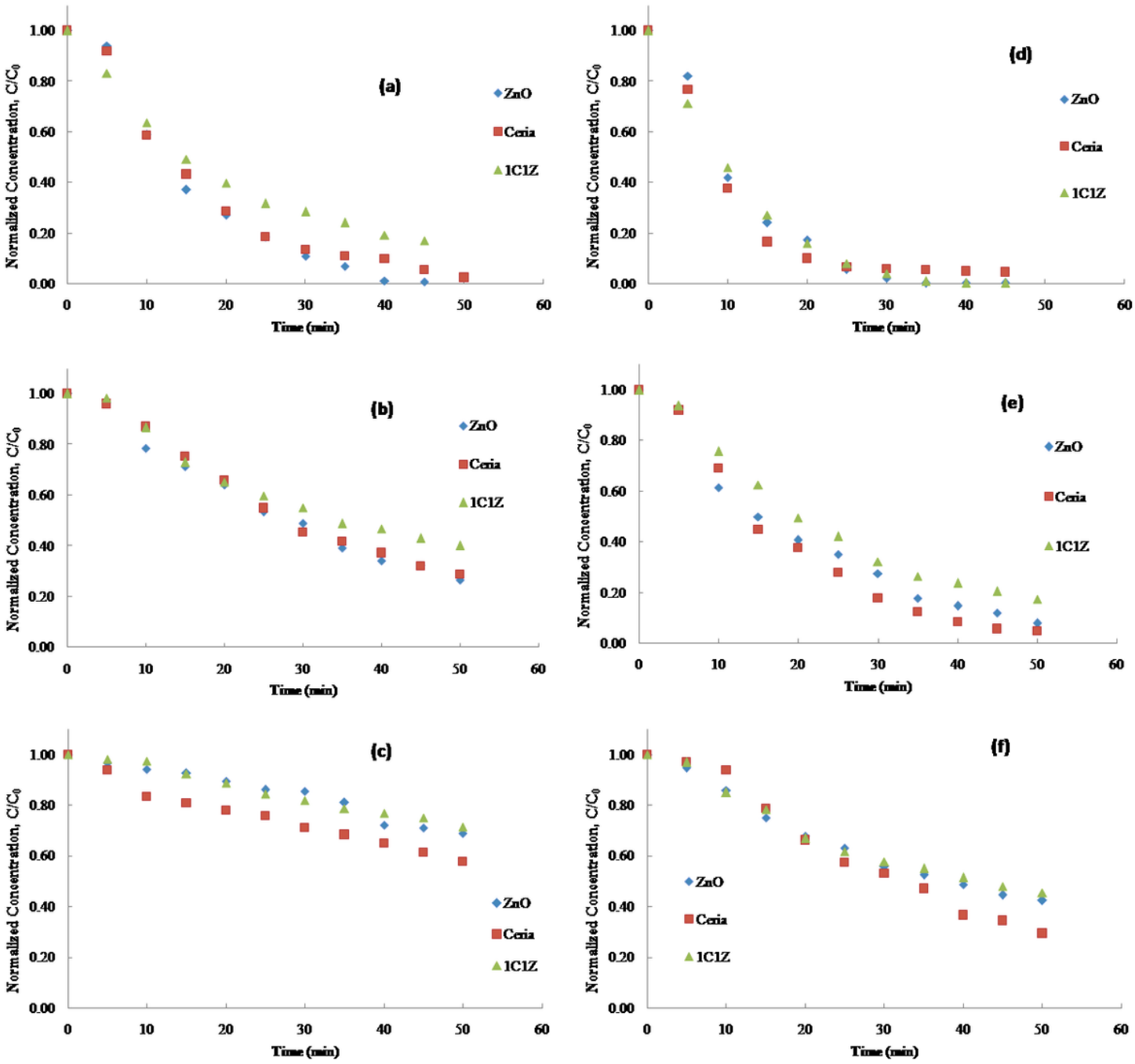

Figure 8

Effect of catalyst loading on RB degradation for catalyst loading of 0.5 g/L (a-c) and 1.5 g/L (d-f). (a& d) RB = 250 mg/L; (b & e) RB = 500 mg/L; (c & f) RB = 1000 mg/L.

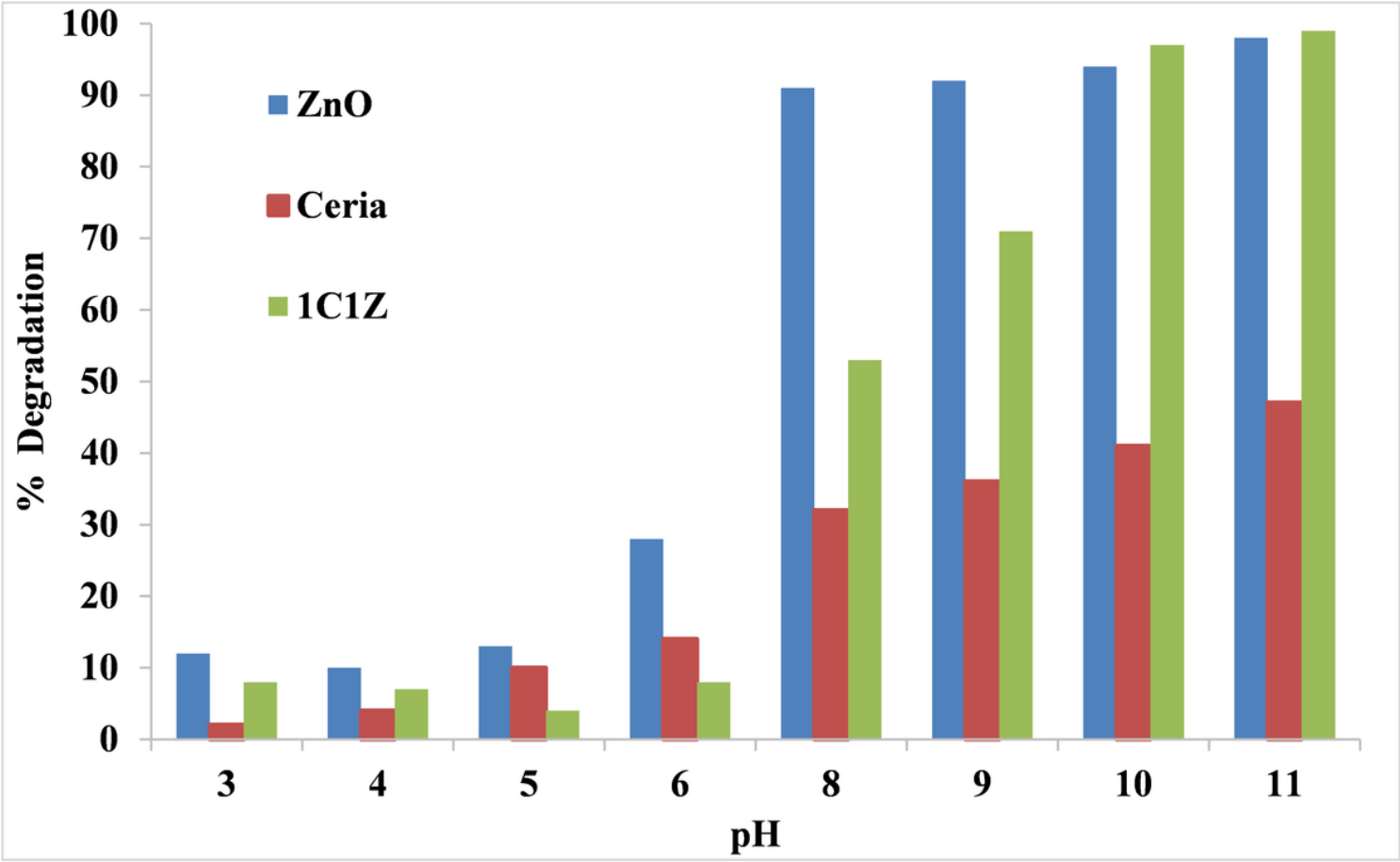

Figure 9

Effect of pH on RB degradation [RB] = 1000 mg/L, catalyst loading = 1 g/L.